Theory of atom transfer with a scanning tunneling microscope

Shiwu Gao, M. Persson, and B. I. Lundqvist
Department of Applied Physics, Chalmers University of Technology and Göteborg University, S-412 96 Göteborg, Sweden
(Received 23 February 1996; revised manuscript received 26 August 1996)

We present and discuss in detail a theory for atom transfer (or bond breaking) using the tip of a scanning tunneling microscope that was outlined by us [Solid State Commun. **84**, 271 (1992)]. The theory is applied to an atomic switch [Nature **352**, 600 (1991)]. In this theory the bond is broken by overcoming the associated potential barrier thanks to a gain in energy from the tunneling electrons. The barrier crossing is described by a truncated harmonic oscillator and the inelastic electron tunneling is modeled by a simple resonance model for the electronic structure. The rate of atom transfer is shown to be Arrhenius-like with a vibrational temperature set by the inelastic tunneling rate. Characteristic features of this mechanism include a crossover from current-driven to thermally activated bond breaking with decreasing applied voltage and a power-law dependence of the bond-breaking rate with the applied voltage, the latter in agreement with experimental findings. We have also identified a current-induced force in the resonance model for tunneling, which in some cases may give an important current-dependent contribution to the potential-energy surface. The general features of our theory should have relevance for many other electronically driven surface processes. [S0163-1829(97)04907-2]

I. INTRODUCTION

One of the most interesting developments in surface science in recent years has been the possibility to manipulate atoms and molecules at a surface on an atomic scale by the tip of a scanning tunneling microscope (STM).[1,2] In particular, the atomic switch realized by Eigler, Lutz, and Rudge,[3] in which a Xe atom is transferred between a Ni surface and a tungsten tip, has attracted much attention in this respect. Our understanding of the detailed physical mechanisms behind these manipulations is rapidly increasing. The theoretical interest stems, to a large part, from the observation of a power-law dependence of the transfer rate as a function of applied voltage.[3] A similar strong power-law dependence has also recently been observed by Shen and co-workers[4] in tip-induced desorption of atomic H on Si surfaces at low applied voltages.

The atom transfer in an atomic switch may be viewed as a potential-barrier crossing problem between the potential wells formed by the interaction of the atom with the tip and the sample, respectively. In the so-called vibrational heating mechanism for atom transfer proposed independently by Gao, Persson, and Lundqvist[5] and Walkup, Newns, and Avouris,[6] the atom overcomes the potential barrier by vibrational activation through a competition between gaining energy from the tunneling current and losing energy to electron-hole pairs and substrate phonons (see Fig. 1). The results obtained in the vibrational heating mechanism for atom transfer explain the key features of the atomic switch and have also been reproduced within a path-integral framework in Ref. 7. For instance, the strong nonlinear dependence of the transfer rate on the applied voltage results from stepwise vibrational excitation of the adsorbate-substrate bond by inelastic electron tunneling.

The importance of nonadiabatic electron processes on bond breaking at surfaces has also been demonstrated in connection with desorption induced by electronic transitions[8] (DIET) and desorption driven by laser-excited hot electrons.[9–11] In particular, the mechanism for laser desorption induced by multiple electronic transitions[12] (DIMET) is closely related to the above mechanism for atom transfer. The prime differences between DIMET and the vibrational heating mechanism lie in the character and the control of the nonequilibrium electron distribution. The possibility of a mechanism analogous to the DIET process in tip-induced bond breaking, in which the barrier crossing occurs via a multistep vibrational excitation induced by a single electron, has been examined by Salam, Persson, and Palmer.[13] In this case the resulting vibrational excitation is a coherent super-

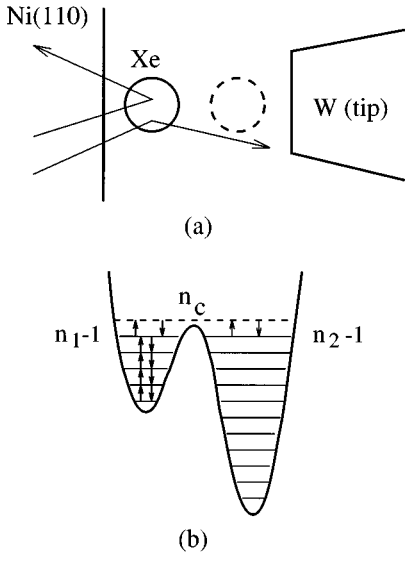

FIG. 1. (a) Schematic picture of the atomic switch. (b) Double-well model for atom transfer based on truncated harmonic oscillators. In the vibrational heating mechanism, the atom transfer results from stepwise vibrational excitation of the adsorbate-substrate bond by inelastic electron tunneling as depicted by arrows between the bound state levels of the adsorption well 1.

position of vibrational states as opposed to an incoherent superposition in the case of the vibrational heating mechanism. Henceforth these two mechanisms will be referred to as the coherent and the incoherent inelastic electron scattering (or tunneling) mechanisms, respectively. The former coherent mechanism has been shown to dominate over the latter incoherent mechanism at such low tunneling currents that the average time between successive electron tunneling events is larger than the vibrational lifetime. In addition, the dependence of the transfer rate on the applied voltage is different in the two cases.

In this paper, we present and discuss in detail the theory for atom transfer (or bond breaking) by incoherent inelastic electron tunneling that was outlined in Ref. 5 and the theory is applied to the atomic switch. The theory is based on the local polaron model[14] and a truncated harmonic-oscillator model for the atom transfer.[15] A key ingredient of the model is that both the nonadiabatic coupling between the ion cores and the electrons and the electron tunneling are assumed to be dominated by the presence of an adsorbate-induced resonance close to the Fermi level. Such a kind of resonance is expected to be a rather general phenomenon[16] and is created when the affinity (or ionization) level of an atom or when the lowest unoccupied (or highest occupied) molecular orbital of a molecule overlaps with the quasicontinuum of levels associated with the surface. The transfer rate is calculated from the Pauli master equation and is shown to follow an Arrhenius-like rate law with a vibrational temperature sustained and controlled by the ratio between the inelastic electron tunneling rate and the vibrational damping rate. We have identified two characteristic features of this mechanism: (i) a crossover from current-driven transfer to thermally activated transfer with increasing temperature or decreasing applied voltage and (ii) a power-law dependence of the transfer rate with applied voltage. Feature (i) has not yet been experimentally identified, whereas (ii) has been observed for the atomic switch and in the tip-induced desorption of atomic H on the Si surface. We have also identified a current-induced force in the resonance model for tunneling, which in some cases may give an important current-dependent contribution to the potential-energy surface.

In Sec. II, we give a detailed account of our theory for bond breaking based on incoherent inelastic electron tunneling. The model is based on the transfer Hamiltonian augmented with a local polaron Hamiltonian and is presented in Sec. II A. The inelastic transition rates between different vibrational levels that are caused by single electron-hole pair and substrate phonon emission and absorption are derived in detail in Sec. II B. How these transition rates have been used to calculate the rate of atom transfer in the truncated harmonic-oscillator model using the Pauli master equation is presented in Sec. II C. The characteristic features of the behavior of the transfer rate are identified and discussed in Sec. II D. The results of the application of the theory to the atomic switch are discussed in Sec. III both with respect to the power-law dependence of the transfer rate on the applied voltage and the direction of transfer. Finally, we give some concluding remarks in Sec. IV.

II. THEORY

A. Transfer Hamiltonian and tunneling conductance

A characteristic feature of the electronic structure of many adsorbates on metal surfaces is the presence of an adsorbate-induced resonance close to the Fermi level.[17] Electron tunneling via such a resonance state has been demonstrated to provide at large tip-sample separations a dominant channel for the current in a STM.[18] We describe this tunneling process by a standard transfer Hamiltonian for the electrons of the combined substrate-adsorbate-tip system as

$$H_e=\sum_k \varepsilon_k c_k^\dagger c_k+\sum_p \varepsilon_p c_p^\dagger c_p+\varepsilon_a c_a^\dagger c_a+\sum_k (t_{ka}c_k^\dagger c_a+\text{H.c.})$$

$$+\sum_p (t_{pa}c_p^\dagger c_a+\text{H.c.}), \tag{1}$$

where k, p, and a label one-electron states $|k\rangle$, $|p\rangle$, and $|a\rangle$ of the sample, the tip, and the adsorbate level, respectively, with corresponding one-electron energies ε_k, ε_p, and ε_a. The last two terms describe the hopping of electrons between the adsorbate and the tip via the adsorbate level. For large tip-substrate distances, $t_{ap}\to 0$ and the Hamiltonian for the adsorbate-substrate electron states reduces to the familiar single-orbital Anderson Hamiltonian. The effects of spin will only be included trivially here by a spin sum that results in factors of 2 at appropriate places. This amounts to a neglect of the potentially important effects of Coulomb correlations among the electrons in a spatial orbital with spin degeneracy that under certain circumstances can lead to Kondo and mixed valence states.[19]

The effect of a bias V between the tip and the substrate is to shift their individual Fermi levels and one-electron energies with respect to each other. The Fermi level ε_{Ft} of the tip is then related to the Fermi level ε_{Fs} of the substrate according to $\varepsilon_{Ft}=\varepsilon_{Fs}-eV$. Note that ε_{Fs} is defined to be fixed, which makes ε_k independent of V, while ε_p, ε_a, t_{ka}, and t_{pa} will in general vary with V.

In the presence of a tip with a bias V, a net tunneling current will be induced between the substrate and the tip. Within the transfer Hamiltonian description, the current from the tip to the sample is given by the well-known expression[20]

$$I_a=2e\frac{2\pi}{\hbar}\sum_{p,k}|T_{pk}|^2[f_s(\varepsilon_k)-f_t(\varepsilon_p)]\delta(\varepsilon_k-\varepsilon_p), \tag{2}$$

where T_{pk} is a T-matrix element and $f_{s,t}(\varepsilon)=1/\{1+\exp[(\varepsilon-\varepsilon_{Fs,Ft})/k_BT]\}$ are Fermi distribution functions. T_{pk} gives the elastic transition amplitude for hopping of an electron from a substrate state k to a tip state p via the adsorbate level a and is given by[21]

$$T_{pk}=t_{pa}G_a^+(\varepsilon)t_{ak}, \tag{3}$$

where $\varepsilon=\varepsilon_k=\varepsilon_p$ and $G_a^+(\varepsilon)=\langle a|(\varepsilon+i0^+-H_e)^{-1}|a\rangle$ is the retarded Green function for the adsorbate level interacting both with the substrate and the tip. In this situation the level interacts with two independent continua of states and the result for $G_a^+(\varepsilon)$ in the Anderson model with a single continuum of states generalizes directly to

$$G_a^+(\varepsilon)=\frac{1}{\varepsilon-\varepsilon_a-\Lambda(\varepsilon)+i\Delta(\varepsilon)}, \tag{4}$$

where $\Delta(\varepsilon)=\Delta_s(\varepsilon)+\Delta_t(\varepsilon)$ and the functions $\Delta_{s,t}(\varepsilon)$ determine the partial widths of the adsorbate level due to the interaction with the substrate and tip, respectively. $\Delta_s(\varepsilon)$ is defined as

$$\Delta_s(\varepsilon)=2\pi\sum_k |t_{ka}|^2\delta(\varepsilon-\varepsilon_k), \tag{5}$$

and similiarly for $\Delta_t(\varepsilon)$. The shift function $\Lambda(\varepsilon)$ is related to $\Delta(\varepsilon)$ via a Hilbert transform. Inserting the result for T_{kp} in Eq. (3) into Eq. (2) for the tunneling current, one obtains readily

$$I_a=\frac{e}{\pi\hbar}\int d\varepsilon[f_s(\varepsilon)-f_s(\varepsilon+eV)]\Delta_t(\varepsilon)\Delta_s(\varepsilon)|G_a^+(\varepsilon)|^2. \tag{6}$$

In this work we shall primarily be concerned with systems where the variation of the adsorbate-induced electronic structure; that is, $G_a^+(\varepsilon)$ is negligible around ε_F over the energy scales eV and k_BT. This implies that the current is linear in the bias, $I_a=\sigma_aV$, and the corresponding elastic tunneling conductance σ_a is given by

$$\sigma_a=\frac{e^2}{\pi\hbar}\Delta_s\Delta_t|G_a^+(\varepsilon_F)|^2, \tag{7}$$

where $\Delta_{s,t}\equiv\Delta_{s,t}(\varepsilon_F)$ are key quantities in the theory. In fact, the measured conductance provides unique information about Δ_t because it is dominated by the elastic channel, whereas Δ_s can be estimated from electronic-structure calculations or photoelectron spectroscopy data measurements on the adsorbate-substrate complex.

B. Inelastic transition rates

1. Electron-hole pairs

In this work we focus on the nonadiabatic resonance coupling between the vibrational motion and the electron-hole pairs since the experience gained from the treatments of electron-hole pair damping of adsorbate vibrations[22,23] and vibrational excitation by inelastic electron tunneling[24] suggests that this coupling is often the dominant mechanism. This coupling is modeled in a standard manner by assuming that $\varepsilon_a(q)$ shifts linearly with the vibrational coordinate q, which results in a total Hamiltonian for the electrons and the adsorbate vibration of the form

$$H=H_e+\hbar\Omega b^\dagger b+\sqrt{\frac{\hbar}{2M\Omega}}(b^\dagger+b)(\varepsilon_a' c_a^\dagger c_a-\varepsilon_{a0}' n_{a00}), \tag{8}$$

where H_e is the transfer Hamiltonian in Eq. (1), Ω is the frequency of the adsorbate vibration with normal coordinate $q=\sqrt{(\hbar/2M\Omega)}(b^\dagger+b)$ and mass M, and $\varepsilon_a'=\partial\varepsilon_a/\partial q$ at $q=0$. The counterterm $-\varepsilon_{a0}' q n_{a00}$, where $n_{a00}=\langle c_a^\dagger c_a\rangle_{V=0}$ is the average occupation of the level a at $V=0$ and $q=0$, and $\varepsilon_{a0}'=\varepsilon_a'$ at $V=0$, ensures that the average force on the oscillator is zero for $V=0$ at $q=0$.

The effect of the electron-vibration interaction, the last term in Eq. (8) denoted by $H_{e\text{-}v}$, on the adsorbate vibration is in general weak and will be treated by first-order perturbation theory. This assumption ignores the possibility of a multiple vibrational excitation by a single electron. The first step is to diagonalize the electronic Hamiltonian H_e as

$$H_e=\sum_\alpha \varepsilon_\alpha c_\alpha^\dagger c_\alpha+\sum_\beta \varepsilon_\beta c_\beta^\dagger c_\beta, \tag{9}$$

where α and β label the stationary electron states $|\alpha\rangle$ and $|\beta\rangle$ on the substrate and the tip side, respectively, with corresponding one-electron energies ε_α and ε_β. These two sets of states are both defined by the Lippmann-Schwinger equation in a similiar way, so it is sufficient to give the definition for one set of states

$$|\alpha\rangle=|k\rangle+(\varepsilon+i0^+-H_e)^{-1}t_{ak}|a\rangle. \tag{10}$$

In terms of the stationary states $|\alpha\rangle$ and $|\beta\rangle$ of H_e, $H_{e\text{-}v}$ is given by

$$H_{e-v}=\varepsilon_a'\sqrt{\frac{\hbar}{2M\Omega}}\sum_{\mu,\nu}(b^\dagger+b)(\langle\mu|a\rangle\langle a|\nu\rangle c_\mu^\dagger c_\nu-n_{a00}), \tag{11}$$

where μ and ν denote any of the stationary one-electron states α and β. The magnitude of the overlap $\langle\mu|a\rangle$ is determined from the local density of the subtrate or tip states for the level a denoted by $\rho_a^s(\varepsilon)$ and $\rho_a^t(\varepsilon)$, respectively. These two functions are defined in a similiar way and, in particular,

$$\rho_a^s(\varepsilon)=\sum_\alpha |\langle\alpha|a\rangle|^2\delta(\varepsilon-\varepsilon_\alpha). \tag{12}$$

As follows directly from Eq. (10), $\rho_a^{s,t}(\varepsilon)$ are given by

$$\rho_a^{s,t}(\varepsilon)=\frac{1}{\pi}\frac{\Delta_{s,t}(\varepsilon)}{[\varepsilon-\varepsilon_a-\Lambda(\varepsilon)]^2+\Delta(\varepsilon)^2}. \tag{13}$$

Thus the magnitudes of the overlaps in Eq. (11) are determined from the width functions and the resonance position.

We need only to calculate excitation and deexcitation rates, as denoted by $\Gamma_\uparrow$ and $\Gamma_\downarrow$, respectively, between the vibrational ground state and the first excited state. This is a direct consequence of the fact that $H_{e\text{-}v}$ is linear in q. It will only induce transitions between nearest-neighboring levels of the harmonic oscillator and all the transition rates can then be expressed in terms of $\Gamma_\uparrow$ and $\Gamma_\downarrow$. In first-order perturbation theory, these transition rates are given by

$$\Gamma_\downarrow=2\frac{2\pi}{\hbar}\sum_{\nu,\mu}|\langle\mu,0|H_{e-v}|\nu,1\rangle|^2 f_\nu(1-f_\mu)\delta(\varepsilon_\mu-\varepsilon_\nu-\hbar\Omega),$$

$$\Gamma_\uparrow=2\frac{2\pi}{\hbar}\sum_{\nu,\mu}|\langle\mu,1|H_{e-v}|\nu,0\rangle|^2 f_\nu(1-f_\mu)\times\delta(\varepsilon_\mu-\varepsilon_\nu+\hbar\Omega), \tag{14}$$

where 0 and 1 denote the vibrational ground state and the first excited state, respectively, and μ and ν denote any of the stationary tip or substrate states with corresponding Fermi distribution functions $f_{\mu,\nu}$. These rates can be decom-

posed into four different terms depending on whether the initial state ν or the final state μ is a tip state α or a substrate state β as

$$\Gamma_{\uparrow,\downarrow}=\Gamma^{ss}_{\uparrow,\downarrow}+\Gamma^{st}_{\uparrow,\downarrow}+\Gamma^{ts}_{\uparrow,\downarrow}+\Gamma^{tt}_{\uparrow,\downarrow}, \tag{15}$$

where the first and second indices in the superscript denote whether the final and initial state belongs to the substrate or the tip.

We shall first evaluate the terms $\Gamma^{ss}_{\uparrow,\downarrow}$ and $\Gamma^{tt}_{\uparrow,\downarrow}$ where the initial and the final states belong to the same electrode. All these terms are similiar, and it is sufficient to evaluate explicitly only the term $\Gamma^{ss}_{\downarrow}$ Inserting the result in Eq. (11) into Eq. (14) gives[22]

$$\begin{aligned}\Gamma^{ss}_{\downarrow}&=2\frac{\pi(\varepsilon'_a)^2}{M\Omega}\sum_{\alpha',\alpha}|\langle\alpha'|a\rangle\langle a|\alpha\rangle|^2[1-f_s(\varepsilon_{\alpha'})]f_s(\varepsilon_\alpha)\\&\quad\times\delta(\varepsilon_{\alpha'}-\varepsilon_\alpha-\hbar\Omega)\\&=2\frac{\pi(\varepsilon'_a)^2}{M\Omega}\int d\varepsilon\rho^s_a(\varepsilon)\rho^s_a(\varepsilon+\hbar\Omega)[1-f_s(\varepsilon+\hbar\Omega)]f_s(\varepsilon)\\&\approx 2\frac{\pi\hbar}{M}(\varepsilon'_a)^2\rho^s_a(\varepsilon_F)\rho^s_a(\varepsilon_F)[1+n(\hbar\Omega)],\end{aligned} \tag{16}$$

where in the first step the sum over states has been replaced with an integral over ε by introducing $\rho^s_a(\varepsilon)$, as defined in Eq. (12). In the last step we have used one of the basic assumption of this work that $\rho^s_a(\varepsilon)$ is essentially constant over an energy scale $eV\gg\hbar\Omega$ and also that the energy integral over $[1-f_s(\varepsilon+\hbar\Omega)]f_s(\varepsilon)$ reduces to $\hbar\Omega[1+n(\hbar\Omega)]$, where $n(\hbar\Omega)=1/[\exp(\hbar\Omega/k_BT)-1]$ is a Bose-Einstein distribution function. In a similiar manner the excitation rate $\Gamma^{ss}_{\uparrow}$ is given by the same expression as for $\Gamma^{ss}_{\downarrow}$ except that $[1+n(\hbar\Omega)]$ is now replaced by $n(\hbar\Omega)$. The same evaluation goes also through for $\Gamma^{tt}_{\downarrow,\uparrow}$, and all these rates can be expressed as

$$\begin{aligned}\Gamma^{ss,tt}_{\downarrow}&=[1+n(\hbar\Omega)]\gamma^{s,t}_{eh},\\\Gamma^{ss,tt}_{\uparrow}&=n(\hbar\Omega)\gamma^{s,t}_{eh},\end{aligned} \tag{17}$$

where

$$\gamma^{s,t}_{eh}=\frac{2\pi\hbar}{M}(\varepsilon'_a)^2\rho^{s,t}_a(\varepsilon_F)^2. \tag{18}$$

In the absence of the tip, γ^s_{eh} reduces to the result for the linewidth broadening γ_{eh} of an adsorbate vibration as obtained by Persson and Persson.[22]

The two remaining terms Γ^{ts} and Γ^{st} in Eq. (15) give the contributions to the transition rates induced by inelastic scattering of tunneling electrons between the substrate and the tip via the adsorbate level. The evaluation of these two terms follows the one of $\Gamma^s_{\downarrow}$ in Eq. (16), but with some important differences. Specifically, the deexcitation rate induced by inelastic tunneling of electrons from the substrate to the tip for positive bias $V>0$ is derived from Eqs. (11) and (14) as

$$\begin{aligned}\Gamma^{ts}_{\downarrow}&=2\frac{\pi(\varepsilon'_a)^2}{M\Omega}\sum_{\alpha,\beta}|\langle\beta|a\rangle\langle a|\alpha\rangle|^2[1-f_t(\varepsilon_\beta)]f_s(\varepsilon_\alpha)\\&\quad\times\delta(\varepsilon_\beta-\varepsilon_\alpha-\hbar\Omega)\\&=2\frac{\pi(\varepsilon'_a)^2}{M\Omega}\int d\varepsilon\rho^s_a(\varepsilon)\rho^t_a(\varepsilon+\hbar\Omega)[1-f_t(\varepsilon+\hbar\Omega)]f_s(\varepsilon)\\&\approx 2\frac{\pi\hbar}{M\Omega}(\varepsilon'_a)^2\rho^t_a(\varepsilon_F)\rho^s_a(\varepsilon_F)eV.\end{aligned} \tag{19}$$

The first step follows the derivation of Eq. (16), while in the last step we have used the basic assumptions of this work: $k_BT\ll|eV|$, $\hbar\Omega\ll|eV|$, and $\rho^{s,t}_a(\varepsilon)$ is essentially constant over an energy scale eV around ε_F. These assumptions imply directly that the excitation rate is equal to the deexcitation rate $\Gamma^{ts}_{\uparrow}=\Gamma^{ts}_{\downarrow}$. For negative bias $V<0$, the Pauli exclusion principle prohibits any inelastic scattering from a substrate state to a tip state with an energy difference $\hbar\Omega$, which forces $\Gamma^{ts}=0$, while the reverse process is allowed and gives a nonzero contribution to Γ^{st}. In fact, time-reversal symmetry and the negligible variation of the electronic structure around ε_F on an energy scale eV imply that the probability for the reversed process is the same as for the direct process when reversing the polarity of V. This gives directly

$$\begin{aligned}\Gamma^{iet}_{\uparrow,\downarrow}&\equiv\Gamma^{ts}_{\uparrow,\downarrow}+\Gamma^{st}_{\uparrow,\downarrow}\\&\approx\frac{2\pi\hbar}{M\Omega}(\varepsilon'_a)^2\rho^t_a(\varepsilon_F)\rho^s_a(\varepsilon_F)|eV|,\end{aligned} \tag{20}$$

and, moreover, from Eq. (18) Γ^{iet} is related to γ_{eh} as

$$\Gamma^{iet}=\frac{|eV|}{\hbar\Omega}\frac{\Delta_t}{\Delta_s}\gamma^s_{eh}. \tag{21}$$

Here we have also used the fact that $\rho^t_a(\varepsilon_F)/\rho^s_a(\varepsilon_F)=\Delta_t/\Delta_s$, which follows directly from Eq. (12). This result shows that a large V, compared to $\hbar\Omega$, can compensate for the weak coupling between the tip and the adsorbate relative to the substrate and result in a Γ^{iet} that may be even larger than γ_{eh}.

2. Phonons

The phonon system of a substrate provides a ubiquitous and important channel for energy transfer between an adsorbate vibration and a substrate. A rather detailed understanding of this process has been established in the field of vibrational spectroscopy.[25] The efficiency of vibrational energy relaxation to the substrate phonon system depends critically on the vibrational frequency relative to the substrate phonon frequencies, the shape of the adsorbate-substrate interaction potential, and the adsorbate-substrate atom mass ratio.

In cases when the adsorbate vibrational frequency is outside the frequency range of the substrate phonon band, the energy transfer to the phonons can only take place via emission and absorption of several phonons through anharmonicity of the adsorbate-substrate bond and becomes typically inefficient if more than two phonons are required. When the adsorbate vibrational frequency overlaps with the substrate phonon band, it turns into a resonance with a temperature independent width $\gamma_{\rm ph}$ determined by single-phonon emis-

sion and absorption. The width will be particularly large and non-Lorenztian line shapes may develop when Ω is of the order of the zone-boundary surface phonon frequencies or larger, whereas at lower frequencies the interaction is weaker due to the decreasing phonon density of states.[26] In this frequency regime the response of the substrate phonon system is in the elastic continuum limit and the following simple expression for $\gamma_{\rm ph}$ (full width at half-maximum) has been derived:[26]

$$\gamma_{\rm ph}=\frac{m}{M}\frac{3\pi}{2\omega_e^3}\Omega^4, \tag{22}$$

where M is the mass of a substrate atom and ω_e is a frequency characterizing the elastic response; $\omega_e\approx 0.8\omega_{\rm max}$ on face-centered-cubic surfaces, where $\omega_{\rm max}$ is the maximum phonon frequency. Note that the strong dependence of $\gamma_{\rm ph}$ on Ω is due to two factors: (i) the adsorbate-substrate force constant $m\Omega^2$ and (ii) the phonon density of states scales as Ω^2. The transition rates between the first excited-state and the ground state level due to emission and absorption of single phonons are then obtained from $\gamma_{\rm ph}$ by including appropriate Bose-Einstein distribution factors as

$$\Gamma_{{\rm ph},\downarrow}=[1+n(\hbar\Omega)]\gamma_{\rm ph},$$
$$\Gamma_{{\rm ph},\uparrow}=n(\hbar\Omega)\gamma_{\rm ph}. \tag{23}$$

3. Total inelastic transition rates

We are now in a position to state one of our main results: the total inelastic transition rates between the vibrational ground state and the first excited state of the adsorbate vibration due to excitation and deexcitation of electron-hole pairs and phonons. In the spirit of first-order perturbation theory, these two different processes contribute additively to the total inelastic transition rates $\Gamma_{\uparrow,\downarrow}$. By collecting the results from Eqs. (17), (20), and (23) one obtains directly

$$\Gamma_\downarrow=[1+n(\hbar\Omega)]\gamma+\Gamma^{iet},$$
$$\Gamma_\uparrow=n(\hbar\Omega)\gamma+\Gamma^{iet}, \tag{24}$$

where $\gamma=\gamma_{eh}+\gamma_{\rm ph}$ and Γ^{iet} is related to γ_{eh} as in Eq. (21). In this expression we have assumed that the coupling of the adsorbate to the substrate is dominating, $\Delta_s\gg\Delta_t$, so that $\gamma_{eh}^s\approx\gamma_{eh}$ and $\gamma_{\rm ph}^s\approx\gamma_{\rm ph}$. Recall the other basic assumptions behind the results in Eq. (24); the local electronic structure of the combined substrate-adsorbate-tip system over an energy scale of eV around ε_F is essentially constant, $k_BT\ll|eV|$, and $\hbar\Omega\ll|eV|$. The form of the total transition rates in Eq. (24) and the fact that Γ^{iet} is linear in V are not specific to our model. Rather they are general features of the incoherent inelastic tunneling mechanism. In fact, this result is also obtained in the theory by Walkup, Newns, and Avouris.[6]

C. Rate of atom transfer

The transfer between the two wells of a double-well potential involves various processes such as thermally activated barrier crossing and tunneling through the barrier. As stressed by Louis and Sethna[27] in the context of atom transfer with the tip of a scanning tunneling microscope, the latter process may, under certain conditions, involve interesting phonon-induced dissipative quantum effects. Here our ambition is to use the simplest possible model that demonstrates in a transparent and sound way the effects of inelastic electron scattering on the transfer rate between the two wells. Therefore we adopt the truncated harmonic-oscillator model for the escape rate out of a single potential well. At the end of this section we shall discuss its applicability to the transfer rate between the two wells of the double-well potential. In particular we argue that this transfer rate is given by the escape rate out of a single well in the situation of a highly asymmetric well.

In the truncated harmonic-oscillator description of the atom transfer, the adsorbate vibrational motion is assumed to be harmonic and the transfer is assumed to occur irreversibly as soon as the atom reaches a vibrational level n with an energy $(n+1/2)\hbar\Omega$ just above the barrier height V_B.[15] The transitions among the different vibrational levels is described by a Pauli master equation, which is justified in the limit of weak inelasticity (i.e., $\Gamma_{\uparrow,\downarrow}\ll\hbar\Omega$). In the prevailing situation of a harmonic oscillator with inelastic couplings that are linear in q, the Pauli master equation reduces to

$$\frac{dP_m}{dt}=(m+1)\Gamma_\downarrow P_{m+1}+m\Gamma_\uparrow P_{m-1}-[m\Gamma_\downarrow+(m+1)\Gamma_\uparrow]P_m. \tag{25}$$

Here $P_m(t)$ is the probability to find the atom in the vibrational state m of the harmonic oscillator at time t and $\Gamma_\uparrow$ and $\Gamma_\downarrow$ are the total inelastic transition rates for vibrational excitation and deexcitation between the vibrational ground state and first excited state, which are specified in Eq. (24).

The solution of this master equation is characterized by two widely separate time scales under the condition[15] that the average number n_v of levels occupied should be less than $\sim n/10$, which, in most situations, is equivalent to $n_v\ll 1$. The two time scales correspond to (i) a rapid relaxation to a quasistationary solution and (ii) a slow decay of this distribution by particles reaching level n and crossing the barrier. Thus the transfer rate R is determined from the quasistationary population of level $n-1$ times the rate for transitions from this level to the level n.

The quasistationary distribution is essentially given by the stationary solution of the master equation in the situation of infinite barrier height. This solution is in general a Boltzmann distribution among the different vibrational levels and is uniquely characterized by a temperature

$$T_v=\frac{\hbar\Omega}{k_B\ln\left(\frac{\Gamma_\downarrow}{\Gamma_\uparrow}\right)}, \tag{26}$$

where we have explicitly inserted the result for the transition rates in Eq. (24). At zero bias, $V=0$, these rates obey detailed balance $\Gamma_\uparrow=\Gamma_\downarrow\exp(-\hbar\Omega/k_BT)$, which yields $T_v=T$ and a vibrational motion that is in thermal equilibrium with the substrate. When a bias is applied between the sample and the tip, the current-induced transition rate Γ^{iet} destroys detailed balance and a nonequilibrium situation is sustained. In fact, T_v will, be higher than T since the ratio $\Gamma_\downarrow/\Gamma_\uparrow$ will, according to Eq. (24), decrease with increasing Γ^{iet}.

Using the Boltzmann expression for the population of the level $n-1$ and the rate of transitions from this level to the level n, $n\Gamma_{\uparrow}$, we arrive at an Arrhenius-like expression for the transfer rate of the form

$$R \simeq n\Gamma_{\uparrow} \exp\left(-\frac{\widetilde{V}_B}{k_B T_v} \right). \tag{27}$$

Here $\widetilde{V}_B$ is defined as $(n-1)\hbar\Omega$ and is close to the actual barrier height V_B. Recall that this expression is valid under the condition $n_v(\hbar\Omega)=1/[\exp(\hbar\Omega/k_B T_v)-1] \ll 1$ or $k_B T_v \ll \hbar\Omega$. This expression for R is the main result of our theory for atom transfer by a tip of a scanning tunneling microscope via stepwise vibrational excitation of the adsorbate-substrate bond by inelastic electron scattering. Moreover, the fact that the population of the levels is close to a Boltzmann distribution characterized by the temperature T_v justifies this mechanism for atom transfer to be called the vibrational heating mechanism. In Sec. II D we shall point out and discuss some characteristic features of this mechanism.

Some caution is needed when applying a model for the escape rate out of a single well to the problem of atom transfer between the two wells of a double well. As has been discussed by Mel'nikov[28] in the classical regime, two additional effects are introduced in the double-well situation: (i) the possibility of rapid recrossing at the top of the barrier, which modifies the escape rate out of a single well, and (ii) a slow back transfer rate of the atom from the other well in which it has first been equilibrated. These two effects are exhibited in the kinetic equation for the populations N_1 and N_2 of wells 1 and 2, respectively, which is given by[28]

$$\frac{dN_1}{dt} = -\widetilde{R}_1 N_1 + \widetilde{R}_2 N_2, \tag{28}$$

$$\frac{dN_2}{dt} = \widetilde{R}_1 N_1 - \widetilde{R}_2 N_2. \tag{29}$$

In the Appendix this kinetic equation is also derived within a simple quantum-mechanical model for the double-well potential simulated by two truncated harmonic oscillators. The rate of atom transfer is readily obtained from Eqs. (28) and (29) to be given by

$$\widetilde{R} = \widetilde{R}_1 + \widetilde{R}_2. \tag{30}$$

The presence of the second well modifies $\widetilde{R}_1$ from the escape rate R_1 out of a single well by a correction factor that is given in the classical limit by[28]

$$\kappa_1 = \frac{\delta_2}{\delta_1 + \delta_2}, \tag{31}$$

where δ_i is the energy loss for an oscillation of the particle in the well i with an energy close to the barrier top. This correction factor is a branching ratio that gives the outcome of the recrossings at the top of the barrier: effect (i) described above. As shown in the Appendix, the correction factor has a similar form in a quantum-mechanical description of the transfer rate for a double-well potential based on truncated harmonic oscillators and is given by

$$\kappa_1 = \frac{W_{2\downarrow}}{W_{1\downarrow} + W_{2\downarrow}}. \tag{32}$$

Here $W_{i\downarrow} = n_i \Gamma_{i\downarrow}$ is the transition rate from the crossing level down to the highest bound level $n_i - 1$ in well i. Effect (ii) for well 1 is generated by the back-rate term $\widetilde{R}_2 N_2$ in the kinetic equation for N_1, Eq. (28). In general, $\widetilde{R}_2$ is related to $\widetilde{R}_1$ through the detailed balance condition

$$\widetilde{R}_2 = \exp\left(-\frac{(E_{02} - E_{01})}{k_B T} \right) \widetilde{R}_1, \tag{33}$$

where E_{01} and E_{02} are the ground-state energies of the two wells.

As we shall see in Sec. III B., the double-well potential for the atomic switch is expected to be highly asymmetric. We argue that this asymmetry validates our description of the atom transfer rate in terms of an escape rate out of an isolated well. In this situation where $(E_{01} - E_{02}) \gg k_B T$ the results in Eqs. (31) and (32) suggest that κ_1 should be close to unity and Eq. (33) shows that $\widetilde{R}_2 \ll \widetilde{R}_1$. Thus we expect $\widetilde{R}$ to be close to R_1.

D. Characteristic features of the incoherent inelastic scattering mechanism

The two prime features of the proposed vibrational heating mechanism for atom transfer are (i) a crossover from current-driven transfer to thermally activated transfer with decreasing bias (ii) a power-law dependence of the transfer on bias. After discussing these two features in turn, we shall also bring up the question about the direction of atom transfer, in particular its relation to the effect of the bias on the potential energy surface.

The Arrhenius-like expression for the transfer rate R in Eq. (27) shows that R is very sensitive to the vibrational temperature T_v. A simple implicit expression for T_v is obtained readily from Eqs. (26) and (24) by introducing Bose-Einstein distribution factors

$$n_v(\hbar\Omega) = n(\hbar\Omega) + \frac{\Gamma^{iet}}{\gamma}. \tag{34}$$

This result shows directly that Γ^{iet}/γ is a key parameter of this theory since it determines the ''heating'' of the vibration above the sample temperature. Depending on the magnitude of this ratio relative to $n(\hbar\Omega)$, the atom transfer may be either in a thermally activated regime $\Gamma^{iet}/\gamma \ll n(\hbar\Omega)$, in a current-driven regime $\Gamma^{iet}/\gamma \gg n(\hbar\Omega)$, or in an intermediate regime $\Gamma^{iet}/\gamma \sim n(\hbar\Omega)$. The current-driven regime is, of course, of prime interest here in controlling the motion along the reaction coordinate.

By varying the control parameters V or T, it is possible to cross over from one regime to the other. For instance, at fixed T the corresponding crossover bias $V^{\star}$ is determined from $n(\hbar\Omega) = \Gamma^{iet}/\gamma$ as

$$V^{\star} = \frac{\hbar\Omega n(\hbar\Omega)}{e} \frac{\gamma}{\gamma_{eh}} \frac{\Delta_s}{\Delta_t}. \tag{35}$$

In the case when $|V| \gg V^{\star}$ the atom transfer is dominated by inelastic electron tunneling, whereas in the opposite case

$|V| \ll V^{\star}$ it is thermally activated. In particular, when $V=0$, the atom transfer is driven by thermal fluctuations and is spontaneous, but with a vanishing rate at low T. Thus, in order to favor current-driven transfer one should have a low T and a large γ_{eh} relative to γ and a strong coupling of the tip to the substrate.

Another important characteristic feature of the proposed mechanism for atom transfer is the power law of the atom transfer rate with bias. This result is evident from the rate expression in Eq. (27) when using the result for T_v in Eq. (26), which leads to

$$\begin{aligned} R &= n\Gamma_{\uparrow}\left(\frac{\Gamma_{\uparrow}}{\Gamma_{\downarrow}}\right)^{n-1} \\ &\simeq n\Gamma^{iet}\left(\frac{\Gamma^{iet}}{\gamma}\right)^{n-1} \\ &\propto V^{n}. \end{aligned} \tag{36}$$

In the second step we have used the explicit expressions for the transition rates in the current-driven regime and the condition $n_v(\hbar\Omega) \ll 1$ behind the Arrhenius expression. In the final step where the power law of R with V is explicitly demonstrated, we have invoked the linear dependence of Γ^{iet} on bias V. The power n is simply the number of levels in the potential well. Note that the power law is caused by the Boltzmann factor $\exp(-V_B/k_BT)$ in Eq. (27) and is thus expected to be a robust result of our model.

Strong deviations from this simple power law can be encountered in a few extreme cases. In the case of strong inelastic electron tunneling, where Γ^{iet} is of the order of γ or larger, the simple Arrhenius expression for the rate behind the result in Eq. (36) breaks down. Another extreme case is encountered when V is so large that $\rho(\varepsilon \pm eV)$ starts to differ appreciably from $\rho(\varepsilon_F)$, so that Γ^{iet} is no longer linear in V. For instance, in the situation of energy- (and bias-) independent $\Delta_{s,t}(\varepsilon)$ corresponding to a Lorentzian form for $\rho_a(\varepsilon)$ and bias-independent ε_a, the maximum rate of vibrational excitation by inelastic tunneling is given by ($V>0$)

$$\begin{aligned} \Gamma^{iet}_{\max} &= 2\frac{\pi(\varepsilon_a')^2}{M\Omega}\int_{\varepsilon_F}^{\infty} d\varepsilon \rho_a^s(\varepsilon)\rho_a^t(\varepsilon+\hbar\Omega) \\ &\simeq \frac{\Delta_t}{\Delta_s}\frac{\pi\Delta}{4\hbar\Omega}\times\begin{cases} \gamma_{eh}, & \tilde{\varepsilon}_a = \varepsilon_F \\ 2\gamma_{eh}\left(\dfrac{\tilde{\varepsilon}_a-\varepsilon_F}{\Delta}\right)^4, & \tilde{\varepsilon}_a-\varepsilon_F \gg \Delta, \end{cases} \end{aligned}$$

where $\tilde{\varepsilon}_a = \varepsilon_a + \Lambda$ and $\gamma_{eh} = \gamma_{eh}^s$ refers to the linewidth broadening at $V=0$ and its value is different in the two limiting cases. In the situation of a half-filled resonance $\tilde{\varepsilon}_a = \varepsilon_F$, Γ^{iet} saturates at a value of $V=\Delta/\pi$ for Γ^{iet}, assuming a linear dependence, whereas for a resonance with a low partial occupation $\tilde{\varepsilon}_a - \varepsilon_F \gg \Delta$, the rapid increase of available density of states on the tip makes Γ^{iet} much larger than the initial γ_{eh}. Except in these two rather extreme cases, the observation of a power-law dependence in the atom transfer should be a strong signature of the incoherent inelastic electron scattering mechanism.

An important issue is the question about how the bias influences the direction of atom transfer. The current-driven atom transfer does not depend directly on the polarity of V since Γ^{iet} depends only on the absolute magnitude of the bias V. The only way the polarity of V can influence the atom transfer rate in this model is through a dependence of the potential-energy surface on the bias.

The transfer Hamiltonian description suggests two different effects of the bias on the interaction energy of the Xe atom with the tip and the sample. In the prevailing situation of a stationary current, the average force F on the adsorbate is, according to the Hellmann-Feynman theorem, given by

$$F = -\left(\frac{\partial \varepsilon_a}{\partial q}\right)_V 2n_a + \varepsilon_{a0}' 2n_{a00}, \tag{37}$$

where $\varepsilon_{a0}' 2n_{a00}$ is the constant counterterm that makes the average force on the adsorbate zero at $q=0$ and $V=0$. n_a is the average occupancy of the orbital a,

$$n_a = \int d\varepsilon [\rho_a^s(\varepsilon) f_s(\varepsilon) + \rho_a^t(\varepsilon) f_t(\varepsilon)]. \tag{38}$$

The bias V will influence n_a and thus F in two different ways. The first effect is that the local electrostatic potential at the adsorbate $\phi(q)$, induced by V, will shift ε_a and in turn change the local density of states on the substrate and tip in Eq. (38). This shift is given by

$$\varepsilon_a = \varepsilon_{a0}(q) - e\phi(q). \tag{39}$$

The second effect is through the change of the occupancy of the orbital a by the change of the tunneling current with V and is governed by $f_t(\varepsilon)$ in Eq. (38).

The nature of these two effects on F is revealed by an expansion of F in Eq. (37) to linear order in V, which gives

$$\begin{aligned} F &\simeq F_0(q) - 2\left[\frac{\partial^2 \varepsilon_a}{\partial V \partial q} n_a + \left(\frac{\partial \varepsilon_a}{\partial q}\right)_V \right. \\ &\quad \left. \times \left\{ \left(\frac{\partial n_a}{\partial \varepsilon_a}\right)_V \left(\frac{\partial \varepsilon_a}{\partial V}\right)_q + \left(\frac{\partial n_a}{\partial V}\right)_{\varepsilon_a} \right\} \right] V \\ &= F_0(q) - \frac{\partial}{\partial q}\left[(-2en_{a0}(q)\phi(q)] - \varepsilon_{a0}'(q) 2\left(\frac{\partial n_a}{\partial V}\right)_{\varepsilon_a} V, \right. \end{aligned} \tag{40}$$

where the subscript 0 indicates that it is the value at $V=0$. The second term of the last line in Eq. (40) describes the force from the interaction of the adsorbate with the electrostatic potential induced by V, whereas the third term of the last line describes the current-induced force from the average occupancy of the orbital a by the tunneling current. Using our explicit results for the local density of states in Eq. (13) and for the tunneling current in Eq. (7), the current-induced force term can be expressed in two different ways

$$F_c = -\varepsilon_{a0}'(q)\frac{\Delta^t}{\Delta^s} 2\rho_a^s(\varepsilon_F) eV \tag{41}$$

$$= -\varepsilon_{a0}'(q)\frac{I_a \hbar}{e\Delta^s}, \tag{42}$$

where $I_a\hbar/e\Delta^s$ is the average occupancy of the orbital a (including spin degeneracy) by the tunneling current. Note that F_c is sensitive to the direction of the current. For instance, F_c has the opposite direction to the tunneling electron current for an affinity level, where $\varepsilon'_{a0}(q)>0$.

An accurate evaluation of the electrostatic force and the current-induced force requires a more detailed description of the electronic structure than is offered by the transfer Hamiltonian, which is primarily tailored to give a good representation of the electronic structure around the Fermi surface. Nevertheless, we think that this model can be used to estimate the magnitude of the current-induced force as done in Sec. III B.

III. RESULTS AND DISCUSSION

We have developed a theory for atom transfer via inelastic electron tunneling in a rather general way because we believe it should be applicable to a wide variety of adsorbates and also to the more general phenomenon of bond breaking. We shall illustrate this theory by applying it to the specific case of the atomic switch, where a rather detailed comparison between theory and experiment is possible.

As we demonstrate below, the atomic switch provides a prototype for inelastic electronic tunneling in atom transfer. The results are divided into two parts: (i) an explanation of the observed power law in the atom transfer rate of the 906-kΩ switch in terms of the number of adsorbate levels in the potential well and (ii) the question about the direction of transfer and its relation to the behavior of the potential-energy surface with bias.

A. Power law of the transfer rate in the 906-kΩ switch

Before making a detailed comparison between theory and experiment, we need to determine the key parameters $\Delta_{s,t}$, γ_{eh}, $\gamma_{\rm ph}$, and N in order to calculate the atom transfer rate. For some of these parameters, we are only able to determine a reasonable range of values, which are consistent with our knowledge about Xe adsorption on metal surfaces.

The parameter Δ_s is estimated from the electronic-structure calculations by Eigler and co-workers[18] of Xe adsorption on a jellium surface. We fit their calculated local density of states for the 6s resonance of the adsorbed Xe atom to a Lorentzian form for $\rho_a^s(\varepsilon)$. This amounts to the approximation that $\Delta_s(\varepsilon)-i\Lambda_s(\varepsilon)$ in Eq. (12) is energy independent. $\rho_a^s(\varepsilon)$ is then given by

$$\rho_a^s(\varepsilon)=\frac{1}{\pi}\frac{\Delta_s}{(\varepsilon-\tilde{\varepsilon}_a)^2+\Delta_s^2}, \tag{43}$$

where $\tilde{\varepsilon}_a=\varepsilon_a+\Lambda_s$ is the resonance energy. The values $\Delta_s=0.6$ eV and $\tilde{\varepsilon}_a-\varepsilon_F=3.5$ eV suggested by this fit indicate that the resonance has only a small occupation and also that the adsorbate-induced electronic structure is essentially constant around the Fermi level for $e|V|\ll\tilde{\varepsilon}_a-\varepsilon_F$. The partial width Δ_t arising from the interaction with the tip can be estimated from the measured tunneling conductance using these resonance parameters and the result for the elastic tunneling conductance in Eq. (7). This gives $\Delta_t\approx 0.2$ eV for the 906-kΩ junction. However, this value should only be viewed as an estimate of the upper limit because there will also be a contribution to the observed tunneling conductance from electrons tunneling directly between the tip and the sample. The existence of this contribution is corroborated from a more detailed theoretical analysis by Cerdá and co-workers[29] of the tunneling current.

The linewidths γ_{eh} and $\gamma_{\rm ph}$ of the Xe vibration due to emission and absorption of electron-hole pairs and phonons, respectively, are estimated in the following manner. The value for the linewidth γ_{eh} is taken from the analysis by Persson[30] of the measured surface resistivity induced by Xe adsorption on Ag, which gives $\gamma_{eh}\sim 3.3\times 10^8$ s^{-1}. Note that this value should only be viewed as an order of magnitude estimate since this kind of measurement gives only information about the lateral Xe vibration on a different surface. The analysis by Persson shows also that the deduced value of γ_{eh} can only be accounted for in a resonance model for the electron-vibration coupling involving a partially occupied 6s resonance. The linewidth $\gamma_{\rm ph}$ of the Xe vibration due to emission and absorption of single phonons, on the other hand, can be calculated directly using Eq. (22) since its vibrational energy is expected to be small compared to the maximum phonon energy of about 36 meV for Ni. No direct information is available on the value of $\hbar\Omega$ for Xe adsorbed on Ni and we have used the value $\hbar\Omega\approx 4$ meV, as suggested by the measured frequency of the perpendicular vibration of Xe in a monolayer on Pt.[31] This value for $\hbar\Omega$ gives a value $\gamma_{\rm ph}=3\times 10^{10}$ s^{-1}, which is about *two orders of magnitude* larger than γ_{eh}.

An estimate of n, the number of levels in the potential well of Xe adsorbed on Ni, requires information about the potential barrier of the double-well potential of the Xe atom between the Ni sample and the tip. The corresponding barrier height V_B can be estimated from calculations of the physisorption interaction energy of Xe with the sample and the tip that we shall return to later on in this section. At this point, it is sufficient to use the information that the diffusion barrier for the lateral motion of Xe on Pt (Ref. 32) is ~ 30 meV, which gives an upper limit of V_B since this diffusion process competes with atom transfer. This consideration suggests that $n<5-7$.

Now we are in a position to calculate the transfer rate and make a detailed comparison with experiments. Figure 2 depicts the calculated transfer rates by numerically integrating the master equation for the potential wells with $n=4$, 5, and 6 vibrational levels, respectively, using the values for the parameters given above and $T=0$ K. These rates show a power-law dependence on the bias with powers 3.89, 4.87, and 5.85, which are close to their respective values of n. This behavior confirms the expected result in the current-driven regime for the power-law dependence, as discussed in Sec. II D. In fact, for this set of parameters, we find from Eq. (34) that $T_v<14$ K for this range of V and the necessary condition $n_v(\hbar\omega)\ll 1$ behind the result for the power law in Eq. (36) is fulfilled. Hence the vibrational heating mechanism is able to reproduce the observed power-law dependence with the power 4.9 ± 0.2 in the 906-kΩ atomic switch in the situation of five levels in the potential well for a Xe atom on the Ni(110) surface. The corresponding barrier height of about 20 meV, which we believe to be a very reasonable value. It is lower than the value of the barrier for the lateral diffusion along the surface and is also consistent with simple modeling

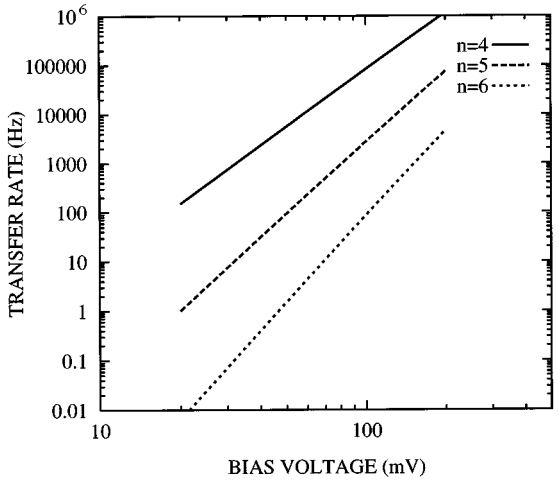

FIG. 2. Calculated atom transfer rates R for various numbers n of levels in the potential well at zero temperature. $\hbar\Omega = 4$ meV, $\gamma_{eh}=3.3\times10^{8}\ \mathrm{s}^{-1}$, $\gamma=3\times10^{10}\ \mathrm{s}^{-1}$, $\Delta_s=0.6$ eV, and $\Delta_t=0.2$ eV.

of the potential-energy surface for Xe interacting with both the sample and the tip, as discussed later in connection with the question about the direction of transfer. Moreover, this barrier height is expected to increase with increasing tip-sample separations and explains the observed competition between the lateral diffusion process and the atom transfer in atomic switches with larger resistance, that is, larger tip-surface separations.[3]

We shall now demonstrate that the proposed set of parameters is consistent with both the observed magnitude of the atom transfer rate and the fact that the thermal activation is negligible at $T=4$ K. In Fig. 3 the calculated transfer rate for the $N=5$ case is shown for three different values of Δ_t. The observed magnitude of the transfer is well reproduced for the value $\Delta_t=0.04$ eV. This value is consistent with the upper limit of ~0.2 eV set by the measured tunneling conductance and indicates that only a minor fraction of the current passes

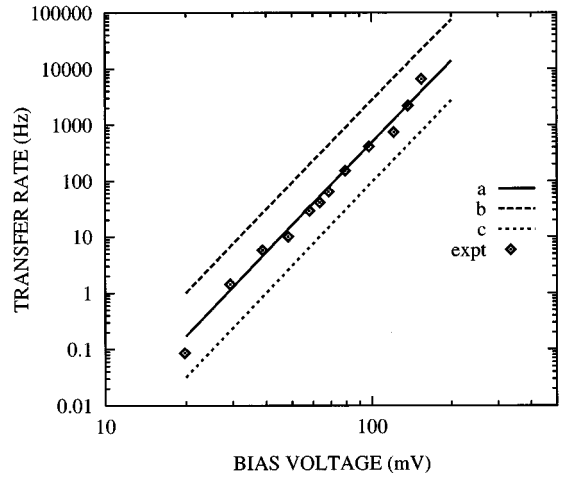

FIG. 3. Calculated atom transfer rate R for various values of the partial width Δ_t compared with the observed transfer rate for the atomic switch at $T=4$ K. The calculated results are based on $n=5$; $\Delta_t/\Delta_s=0.07$ (a), 0.1 (b), and 0.05 (c), respectively; and otherwise the same values for the parameters as in Fig. 2. The experimental data are taken from Eigler, Lutz, and Rudge (Ref. 3).

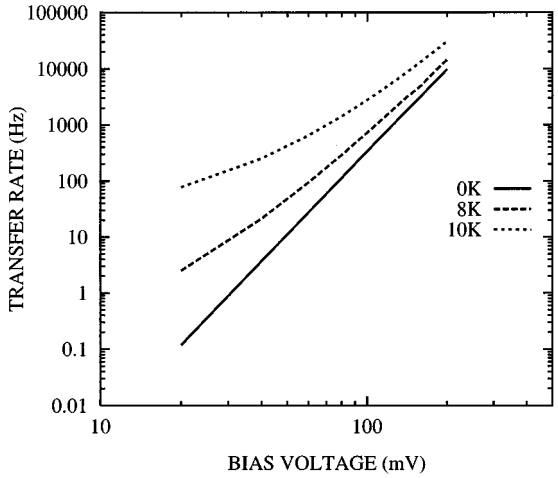

FIG. 4. Temperature dependence of the calculated transfer rate R. The results are based on $N=5$, $\Delta_t/\Delta_s=0.07$, and otherwise the same values for the parameters as in Fig. 2.

via the resonance. Moreover, $\Delta_t=0.04$ eV leads to $\Delta_t/\Delta_s\sim0.07$, a value that is also consistent with the assumption behind the results for the transition rates that the interaction of the atom with the tip should be small compared to its interaction with the substrate. In the expression for Γ^{iet} the small value for the ratio Δ_t/Δ_s is compensated for by the large factor $e|V|/\hbar\Omega$, with the net result $\Gamma^{iet}\sim4\gamma_{eh}$ at $V\sim0.2$ V, but is still much less than $\gamma\approx\gamma_{\mathrm{ph}}\sim10^{2}\gamma_{eh}$. However, the value of the ratio Γ^{iet}/γ is still sufficiently large so that for the range of biases of interest the atom transfer is in the current driven regime at the temperature $T=4$ K of the experiment. This is evident from the fact that the crossover bias $V^{\star}$, as defined in Eq. (35), where thermal activation and inelastic electron tunneling are equal contributors, is below the threshold for vibrational excitation by the current.

The effect of varying the temperature on the calculated atom transfer rate is shown in Fig. 4. As the temperature is elevated, the thermally activated regime, as characterized by a constant R, increases in range over V. For instance, already at $T=8$ K, R starts to deviate substantially from a power-law behavior in the range of V of interest in the experiment. This behavior of R with T constitutes a definite prediction of the vibrational heating mechanism that could be tested experimentally. At zero bias, transfer can be induced by thermal fluctuations, which has also been reported in the atomic switch experiment at closer tip-sample separation where V_B is expected to be smaller.

Finally, we comment on the possibility of Xe atom transfer via coherent inelastic electron tunneling. This process has been shown by Salam, Persson, and Palmer[13] to dominate at small tunneling currents I through the resonance well below the characteristic current $I^{\star}=C_N e\gamma$. In the case of the 906-k Ω switch, the calculated value for $\gamma\approx\gamma_{\mathrm{ph}}$ and $c_2\approx2$ gives $I^{\star}\approx10$ nA, and based on the suggestion that about 20% passes through the resonance, this mechanism should start to be dominating for V well below 50 mV. Thus this mechanism may be an important contributor to Xe atom transfer in the 906-kΩ switch at low biases.

B. Direction of Xe transfer

The experiments show clearly that the Xe atom can be transferred reversibly between the tip and the sample by applying voltage pulses ± 0.8 V and the direction of Xe transfer is in the direction of the electron current. In the lower range of biases, as used in the measurements of the transition rate, the Xe transfer is also in the direction of the electron current, but, to the best of our knowledge, results have only been reported for positive bias in this situation. We now discuss the direction of the Xe transfer in terms of the potential-energy surface (PES) and its bias dependence.

There have been several attempts by differents groups[6,33,34] to model the PES of a Xe atom between the W tip and the Ni surface using empirical potentials. The parameters are chosen in different ways, but all these PES constructions give rise to a highly asymmetric double-well potential with a barrier height that increases with increasing tip-sample distance. The potential well is deeper on the tip side, which is consistent with larger experimental adsorption energy D of Xe on W than on Ni: $D(\mathrm{Ni}) \approx 240$ meV (Ref. 35) and $D(\mathrm{W}) \approx 350$ meV (Ref. 36), and also with the observation that there is an irreversible and spontaneous transfer of the Xe atom from the sample to the tip at small tip-sample distances. At distances in a range suggested by experiments, the barrier height is in the range 5–30 meV. Another consensus of all this work is the finding that the dipole interaction term explains the observed direction of Xe transfer when applying large voltage pulses ± 0.8 V. The electrostatic interaction of the electric field with the large dipole moment of $\sim 0.3D$ of the adsorbed Xe atom is sufficiently large to change the asymmetry of the double-well potential at $V=-0.8$ V, leading to Xe transfer from the tip to the sample.

In addition to the dipole interaction as discussed in Sec. II D, the tunneling current may affect the atom transfer by changing the occupancy of the resonance and induce a current-induced force F_c on the atom. We have made an estimate of the magnitude of F_c using the transfer Hamiltonian by comparing its magnitude at the equilibrium position with the electrostatic force F_{el} induced by the charge-transfer into the 6s resonance of the Xe atom upon adsorption. Note that the simple charge-transfer model is too naive to describe the adsorbate-induced dipole moment for Xe adsorbed on a metal surface; it gives the wrong sign of the dipole moment. The force F_{el} is simply given by the electric field at the adsorbate times the net charge $-e2n_a^0$ on the adsorbate. The ratio between these two forces is given by

$$\left|\frac{F_c}{F_{\mathrm{el}}}\right| = \frac{|\varepsilon_a'|\,\frac{\Delta^t}{\Delta^s}\rho_a(\varepsilon_F)d}{n_a^0}, \tag{44}$$

where the distance d between the tip and substrate enters though the estimate V/d for the electric field at the adsorbate. Using the values for the resonance parameters and $d \sim 5$ a.u., the value of the numerator is ~ 0.015. The occupancy n_a^0 at zero bias can be directly estimated from the local density of states of the 6s resonance of Xe as

$$n_a^0 = \int_{-\infty}^{\varepsilon_F} d\varepsilon \frac{1}{\pi} \frac{\Delta}{(\varepsilon - \tilde{\varepsilon}_a)^2 + \Delta^2} \simeq \frac{1}{\pi} \frac{\Delta}{\tilde{\varepsilon}_a - \varepsilon_F}. \tag{45}$$

Our estimated values for the 6s resonance parameters gives $n_a^0 \approx 0.055$. Thus the current-induced force F_c is about a factor 3 less than the electrostatic force F_{el} at the equilibrium position in our model.

IV. CONCLUDING REMARKS

We have given a detailed presentation and discussion of a theory for tip-induced atom transfer (or bond breaking) by inelastic electron tunneling. This theory was outlined by us and applied to the atomic switch in Ref. 5. The atom transfer is viewed as a potential-barrier-crossing problem and is modeled by a one-dimensional truncated harmonic oscillator. The inelastic tunneling by a single electron is assumed to induce only stepwise transitions between the different vibrational levels and the corresponding rates have been calculated within a simple resonance model of the electronic structure. This assumption has previously been shown to be valid in situations where the resonance tunneling rate is much larger than the vibrational lifetime.

The rate of atom transfer is shown to follow an Arrhenius-like rate law with a vibrational temperature sustained and controlled by the ratio of the inelastic electron tunneling rate to the vibrational damping rate. We have identified two characteristic features of this mechanism: (i) a crossover from current-driven transfer to thermally activated transfer with decreasing applied voltage and (ii) a power-law dependence of the transfer rate with applied voltage. Feature (i) has not yet been observed, while (ii) has been observed for the atomic switch and in the tip-induced desorption of atomic H on Si surface. We have also identified a current-induced force in the resonance model for tunneling, which in some cases may give an important current-dependent contribution to the potential-energy surface. Although here discussed for the atomic switch, the general features of our theory should have relevance for many other electronically driven surface processes.

ACKNOWLEDGMENTS

This work is supported by the Swedish Natural Science Research Council (NFR) and the National Board for Industrial and Technical Development (NUTEK).

APPENDIX

In this appendix we extend the truncated oscillator model for the escape rate out of a single well to the transfer rate between the two wells of a double-well potential. In this model we derive the kinetic equations, Eqs. (28) and (29), for the populations of the two wells and the correction factor in Eq. (32). We begin with a discussion of the escape rate out of a single well.

As demonstrated by Montroll and Shuler many years ago, the escape rate out of a truncated harmonic oscillator is given by the smallest eigenvalue of the transition matrix in the master equation.[15] In this model the well is represented by a truncated harmonic oscillator with n levels and the particle is

assumed to escape promptly as soon as it reaches level n.

The time dependence of the probability P_k to find the particle in level k is governed by the master equation

$$\frac{dP}{dt} = -WP, \tag{A1}$$

where $P=(P_0,P_2,\ldots,P_n)$ and W is the transition matrix. Note that we have defined the transition matrix with a negative sign. The solution of the master equation is determined by the eigenvalues and eigenvectors of W. Because of the detailed balance condition

$$W_{kk'} = \exp[-\beta(E_k - E_{k'})]W_{k'k}, \tag{A2}$$

where $-W_{kk'}$ is the transition rate from level k' to k, $\beta = 1/k_BT$, and E_k is the energy of level k, W is nonsymmetric and the eigenvectors do not form an orthogonal set.

This problem is remedied either by a symmetrization, as done originally by Montroll and Shuler,[15] or by redefining the scalar product as done here. We define the scalar product as

$$\langle P,Q\rangle = \sum_k Z\exp(\beta E_k)P_kQ_k, \tag{A3}$$

where $Z=\Sigma_k e^{-\beta E_k}$ is the partition function, so that the condition of detailed balance, Eq. (A2), implies that W is Hermitian under this scalar product, that is, $\langle P,WQ\rangle = \langle WP,Q\rangle$. Thus the normalized eigenvectors P_μ of W with eigenvalues w_μ are orthogonal under this scalar product and form a complete set, in which the solution to Eq. (A1) can be expanded as

$$P(t) = \sum_\mu \exp(-w_\mu t)\langle P_\mu, P(t=0)\rangle P_\mu. \tag{A4}$$

In the situation, when the smallest eigenvalue w_0 is well separated from the other ones, the population $N=\Sigma_k P_k$ obeys a simple rate equation with the rate w_0.

For low temperatures $\beta\hbar\Omega \ll 1$, Montroll and Shuler have shown that the smallest eigenvalue of W is well separated from the other ones and it can be calculated perturbatively when taking the transition rate from level $n-1$ to n as a perturbation. This perturbation is given by

$$\delta W_{k'k} = W_{n,n-1}\delta_{k'n-1}\delta_{kn-1}. \tag{A5}$$

The smallest eigenvalue of the unperturbed system $w_0^{(0)}=0$ and the associated normalized eigenvector $P_{0,k}^{(0)}$ is given by the stationary thermal probability distribution

$$P_{0,k}^{(0)} = Z^{-1}\exp(-\beta E_k). \tag{A6}$$

Hence, from first-order perturbation theory the rate R for the population $N(t)=\langle P_0,P(t)\rangle$ is given by

$$R = \langle P_0^{(0)}, \delta W P_0^{(0)}\rangle \simeq W_\uparrow \exp[-\beta(E_{n-1}-E_0)]. \tag{A7}$$

Because we are considering the low-temperature limit, we have made the approximation $Z\simeq\exp(-\beta E_0)$ and in addition introduced the notation $W_\uparrow = W_{n,n-1}$. This expression is a well-known result for the escape rate out of a single well in the truncated harmonic-oscillator model, as obtained by Montroll and Shuler.[15] It is the same as in Eq. (27) in Sec. II C.

A simple extension of the truncated oscillator model for the escape rate out of a single well to the transfer rates between the two wells of a double-well potential is obtained by representing also the second well by a truncated oscillator and letting the energy levels close to the potential barrier between the two wells be represented by a single crossing level. The transfer rate between the two wells of this model can now be calculated using the same methodology. As shown schematically in Fig. 1(b), the model consists now of three parts: two truncated oscillators with n_1 and n_2 bound states at the two sides and the crossing level n_c. The transition rates between the crossing level n_c and the highest bound levels n_1-1 and n_2-1 of wells 1 and 2, respectively, are now treated as a perturbation. The unperturbed system has now three degenerate eigenvectors with eigenvalues equal to zero. Two of these vectors represent the stationary thermal distributions of the isolated wells and are given in normalized form by

$$P_{1k}^{(0)} = \begin{cases} \dfrac{e^{-\beta E_k}}{\sqrt{ZZ_1}} & \text{in well 1} \\ 0 \quad \text{for } k=n_c \text{ or in well 2,} \end{cases}$$

$$P_{2k}^{(0)} = \begin{cases} \dfrac{e^{-\beta E_k}}{\sqrt{ZZ_2}} & \text{in well 2} \\ 0 \quad \text{for } k=n_c \text{ or in well 1,} \end{cases} \tag{A8}$$

whereas the third normalized eigenvector represents a stationary distribution on the crossing level and is given by

$$P_{3k}^{(0)} = \begin{cases} \dfrac{e^{-\beta E_{n_c}/2}}{\sqrt{Z}} & \text{for } k=n_c \\ 0 \quad \text{otherwise.} \end{cases} \tag{A9}$$

In Eqs. (A8) and (A9), Z_1 and Z_2 are the partition functions of the isolated wells 1 and 2, respectively, and Z is that of the whole system. We can now calculate the transfer rate using first-order degenerate perturbation theory in the subspace spanned by $P_1^{(0)}$, $P_2^{(0)}$, and $P_3^{(0)}$. The secular equation for the eigenvalue w reads

$$\begin{aligned} wP_1^{(0)} &= \langle P_1^{(0)}, \delta W P_1^{(0)}\rangle P_1^{(0)} + \langle P_1^{(0)}, \delta W P_3^{(0)}\rangle P_3^{(0)}, \\ wP_2^{(0)} &= \langle P_2^{(0)}, \delta W P_2^{(0)}\rangle P_2^{(0)} + \langle P_2^{(0)}, \delta W P_3^{(0)}\rangle P_3^{(0)}, \\ wP_3^{(0)} &= \langle P_3^{(0)}, \delta W P_1^{(0)}\rangle P_1^{(0)} + \langle P_3^{(0)}, \delta W P_2^{(0)}\rangle P_2^{(0)} \\ &\quad + \langle P_3^{(0)}, \delta W P_3^{(0)}\rangle P_3^{(0)}, \end{aligned} \tag{A10}$$

where δW is the perturbation matrix, that is, the matrix of transition rates between the crossing level n_c and the two wells, as shown in Fig. 1. One of the three solutions to the secular matrix has a large eigenvalue that is of the same magnitude as the transition matrix elements and is not of interest here. This solution is disregarded by eliminating $P_3^{(0)}$ from Eq. (A10) and the resulting equation is given by

$$wP_1^{(0)} = \delta W_1^{\rm eff} P_1^{(0)} - \delta W_{12}^{\rm eff} P_2^{(0)},$$

$$wP_2^{(0)} = -\delta W_{21}^{\rm eff} P_1^{(0)} + \delta W_2^{\rm eff} P_2^{(0)}. \quad \text{(A11)}$$

The effective transition matrix elements of $\delta W^{\rm eff}$ in Eq. (A11) are given by

$$\delta W_1^{\rm eff} = \frac{W_{1\uparrow} W_{2\downarrow}}{W_{1\downarrow} + W_{2\downarrow}} \frac{\exp(-\beta E_{n_1-1})}{Z_1}, \quad \text{(A12)}$$

$$\delta W_2^{\rm eff} = \frac{Z_1}{Z_2} \delta W_1^{\rm eff}, \quad \text{(A13)}$$

$$\delta W_{12}^{\rm eff} = \delta W_{21}^{\rm eff} = \sqrt{\frac{Z_2}{Z_1}} \delta W_1^{\rm eff}, \quad \text{(A14)}$$

where $W_{i\uparrow}$ and $W_{i\downarrow}$ are the transition rates from the highest bound level of well i to the crossing level and for the reverse transition, respectively. We have also neglected w in the effective transition matrix elements because the values of w of interest are much smaller than the matrix elements in Eq. (A10).

The results of Eq. (A11) for the populations $N_1(t)$ and $N_2(t)$ of the two wells are identical to that of the kinetic equation in Eq. (28): $N_i(t) = \langle P_i^{(0)}, P(t) \rangle$ and $\tilde{R}_i = \delta W_i^{\rm eff}$ for $i = 1,2$. An inspection of Eq. (A12) shows that $\tilde{R}_1$ differs from the single-well result in Eq. (A7) by the factor

$$\kappa = \frac{W_{2\downarrow}}{W_{1\downarrow} + W_{2\downarrow}}, \quad \text{(A15)}$$

which proves the result in Eq. (32). The relation in Eq. (A13) is also valid between $\tilde{R}_2$ and $\tilde{R}_1$. It is a statement of the detailed balance condition in Eq. (33) in the low-temperature limit because $Z_1/Z_2 = \exp[-\beta(E_{01} - E_{02})]$ in this limit.

[1] See articles in *Atomic and Nanometer Scale Modifications of Materials: Fundamentals and Applications*, edited by Ph. Avouris (Kluwer, Dordrecht, 1993).

[2] J. A. Stroscio and D. M. Eigler, Science **254**, 1319 (1991).

[3] D. M. Eigler, C. P. Lutz, and W. E. Rudge, Nature **352**, 600 (1991).

[4] T.-C. Shen, C. Wang, G. C. Abeln, J. R. Tucker, J. W. Lyding, Ph. Avouris, and R. E. Walkup, Science **268**, 1590 (1995).

[5] Shiwu Gao, M. Persson, and B. I. Lundqvist, Solid State Commun. **84**, 271 (1992); J. Electron Spectrosc. Relat. Phenom. **64/65**, 665 (1993).

[6] R. E. Walkup, D. M. Newns, and Ph. Avouris, Phys. Rev. B **48**, 1858 (1993); J. Electron Spectrosc. Relat. Phenom. **64/65**, 523 (1993).

[7] M. Brandbyge and P. Hedegård, Phys. Rev. Lett. **72**, 2919 (1994).

[8] See, for instance, *DIET V*, edited by E. B. Stechel and D. R. Jennison (Springer, Berlin, 1993).

[9] D. M. Newns, T. F. Heinz, and J. A. Misewich, Prog. Theor. Phys. Suppl. **106**, 411 (1992).

[10] S. Gao, B. I. Lundqvist, and W. Ho, Surf. Sci. **341**, L1031 (1995).

[11] J. A. Misewich, T. F. Heinz, P. Weigand, and A. Kalamarides, in *Laser Spectroscopy and Photochemistry on Metal Surfaces*, edited by H. L. Dai and W. Ho (World Scientific, Singapore, 1995).

[12] J. A. Prybyla, T. F. Heinz, J. A. Misewich, M. M. T. Loy, and J. H. Glownia, Phys. Rev. Lett. **64**, 1537 (1990).

[13] G. P. Salam, M. Persson, and R. E. Palmer, Phys. Rev. B **49**, 10 655 (1994).

[14] J. W. Gadzuk, Phys. Rev. B **44**, 13 466 (1991).

[15] E. W. Montroll and K. E. Shuler, Adv. Chem Phys. **1**, 361 (1958).

[16] For a recent review see, e.g., B. I. Lundqvist, in *Electron Processes at Solid Surfaces*, edited by E. Ilisca and K. Makoshi (World Scientific, Singapore, in press).

[17] N. D. Lang, Comments Condens. Matter. Phys. **14**, 253 (1989).

[18] D. M. Eigler, P. S. Weiss, E. K. Schweizer, and N. D. Lang, Phys. Rev. Lett. **66**, 1189 (1991).

[19] See, e.g., G. D. Mahan, in *Many Particle Physics* (Plenum, New York, 1990), p. 957.

[20] See, e.g., G. D. Mahan, in *Many Particle Physics* (Plenum, New York, 1981), p. 798.

[21] See, e.g., *Advanced Quantum Theory*, edited by P. Roman (Addison-Wesley, Reading, MA, 1965), Chap. 4.

[22] B. N. J. Persson and M. Persson, Solid State Commun. **36**, 175 (1980).

[23] M. Persson and B. Hellsing, Phys. Rev. Lett. **49**, 662 (1982).

[24] B. N. J. Persson and A. Baratoff, Phys. Rev. Lett. **59**, 339 (1987).

[25] D. C. Langreth and M. Persson, in *Laser Spectroscopy and Photochemistry on Metal Surfaces* (Ref. 11), p. 498.

[26] J. A. Leiro and M. Persson, Surf. Sci. **207**, 473 (1989).

[27] A. A. Louis and J. P. Sethna, Phys. Rev. Lett. **74**, 1363 (1995).

[28] V. I. Mel'nikov, Phys. Rep. **209**, 1 (1991).

[29] J. R. Cerdá, P. L. de Andres, F. Flores, and R. Perez, Phys. Rev. B **45**, 8721 (1992).

[30] B. N. J. Persson, Phys. Rev. B **44**, 3277 (1991).

[31] K. Kern, R. David, R. L. Palmer, and G. Comsa, Phys. Rev. Lett. **56**, 2823 (1986).

[32] K. Kern, P. Zeppenfeld, and G. Comsa, Surf. Sci. **195**, 353 (1988).

[33] P. L. de Andres, F. Flores, J. R. Cerda, and P. M. Echenique, J. Phys.: Condens. Matter. **5**, A411 (1993).

[34] J. J. Saenz and N. Garcia, Phys. Rev. B **47**, 7537 (1993).

[35] K. Christmann and J. E. Demuth, Surf. Sci. **120**, 291 (1982).

[36] J. T. Yates and N. E. Erickson, Surf. Sci. **64**, 43 (1974).